A. Balandin, G. Jin, and K.L. Wang, *J. Electronic Materials*, **29**, 549-553 (2000).

Issues of Practical Realization of a Quantum Dot Register for Quantum Computing

Alexander Balandin
Department of Electrical Engineering
University of California – Riverside
Riverside, CA 92521

Gaolong Jin and Kang L. Wang
Device Research Laboratory
Electrical Engineering Department
University of California - Los Angeles
Los Angeles, CA 90095

Abstract

We present a quantum dot structure fabricated by the lithographic positioning, which can be used as a prototype of the quantum dot register for quantum computing. Using simple model calculations we show that parameters of our quantum dot structure are very close to the ones required for two possible embodiments of a quantum computer. Results of numerical simulation of the quantum dot register, as well as discussion of materials and technological issues of fabrication of quantum logic gates are also presented.

I. Introduction

A quantum computer is a device, which uses the quantum states to encode and process information. The elementary unit of quantum information is the *qubit*, which can be envisaged as a 2-state system such as a spin-half particle, a 2-level atom or a quantum dot. Contrary to any classical object, a quantum system can exist not only in the ground state |0> or the excited state |1>, but in any linear superposition of these two states. The possibility of preparing such superposition states, and coherent manipulation of these states provide the main advantage of quantum computers, permitting them to make certain problems, like prime factorization, solvable much faster [1].

The progress in experimental development of quantum logic gates on the basis of solid-state structures has been rather slow. This is primarily due to the following factors: (i) the decoherence problem, which is inherently more severe for solid state systems [2]; (ii) difficulties in fabrication of high quality quantum dot arrays with precise control of dot size and position; and (iii) difficulties of addressing individual qubits which formed by electronic confined states in a quantum dot [3] or by spin states in a bulk semiconductor [4]. Until recently, research work on the solid-state embodiments of a quantum computer has been pure theoretical. Currently, the situation began to change owing to several most recent technological achievements. It is now possible to proceed with practical issues of solid-state implementation of the quantum computing logic gates.

II. Recent technological breakthroughs

Several recent technological achievements in fabricating quantum dots, and progress in optical measurement techniques have made a solid-state quantum computer much more feasible than a couple of years ago.

Unlike optical applications, for which random arrangement of the uniformly sized dots is often sufficient, all envisioned information processing applications of quantum dots require their exact positioning at predetermined locations. A successful lithographic positioning of self-assembled Ge quantum dots of extremely high quality on pre-patterned Si (001) substrate has been finally achieved [5-6]. The uniformly shaped dots were placed in the corners of a lithographically written rectangular mesa. The distance between the dots was kept in a range of 100A – 200A.

Another important development that opens up an opportunity of using quantum dots for quantum computing with optical INPUT/OUTPUT is the detection of a coherent optical signal from individual excitons in a single quantum dot, recently reported by Bonadeo *et al*. [7-8]. The detection was carried out using coherent nonlinear optical spectroscopy of individual excitons in 4 nm wide GaAs quantum dots. The obtained data shows that energy relaxation and dephasing rates are on the order of $T_2=\gamma^{-1}$ ~ 100 ps with the energy splitting between two polarization states E ~ 60 meV. Picosecond optical excitation was used to coherently control the excitation in a single quantum dot on a time scale that is short compared with the time scale for loss of quantum coherence. The results reported in Ref. [7-8] extend the potential of coherent control in semiconductors to the limit of a single quantum system in a zero-dimensional quantum dot.

Demonstrated robust control of few electrons in a quantum dot [9] was another major step toward solid state implementation of a quantum logic gate, since a number of proposed realizations require single or few electron quantum dots [10-12]. Among recent breakthroughs, one should also mention successful growth of InAs quantum dots on Si substrates [13-14].

These technological achievements made it practical to explore in-depth both theoretically and experimentally a feasibility of a quantum dot register for quantum computing. In this paper we present a molecular beam epitaxy (MBE) grown quantum dot array, which can be used as a prototype for quantum computing register. We show that parameters of the presented structure are close to the required for the quantum logic gate operation. Results of the investigation of processes limiting the quantum coherence in quantum dots are also presented.

III. Design and fabrication of the quantum dot register

There are two most popular types of the quantum logic gates on the basis of quantum dots, which have been proposed so far. The first type utilizes the charge of an electron to form a qubit [15-16], while the second one uses electron spin to represent a qubit [4,12]. Both approaches have their own advantages and disadvantages. Spins are usually stronger decoupled from the environment than electronic excitation, and thus it is easier to preserve quantum coherence required for quantum gate operation in a spin system. At the same time, the electron charge (orbital degrees of freedom) can offer convenient gating, and easier addressing of individual qubits. Unlike spin-based systems, they do not require locally applied magnetic field, which is always a technologically challenging task. Provided that we can suppress de-coherence to some degree or drive the computation very fast (faster than the system's de-coherence time), the charge-based computational basis states can be used for quantum information processing. From the quantum dot fabrication point of view, these two types of the logic gates are nearly identical: one requires a quantum dot with one confined level (ground state), while the other usually needs two confined electron states [3,15-16]. Here, we concentrate more on the second one.

Most likely, the working solid-state based quantum computer will combine the classical conventional VLSI circuits with quantum computing units on the same chip to form some sort of a hybrid circuit. This will allow us to overcome the difficulty in maintaining quantum coherency for sufficiently long time. Thus, it is important to consider quantum dots made out of material, which can be easily integrated on Si substrates. Two possible candidates for material systems are Ge and InAs quantum dots grown on Si. The first one is indirect band-gap material while the other one is direct band-gap material. For the quantum computing models, which relay on optical drive and READ/WRITE, the right choice most likely will be the direct band-gap materials. For the models, which are driven entirely by electric means, the type of band-gap is not that important.

As an example, we consider the basic elements of a quantum dot register schematically shown in Fig. 1. The inset to this figure shows the two lowest quantum confined electron states in a quantum dot, which will form computational basis states {|0>,|1>}. These states will be used for information encoding and processing in a coherent way required for quantum computing. A complete logic unit (quantum circuit) will require several closely spaced arrays of quantum dots as shown in Fig. 1. The principle of operation of a quantum dot-based quantum logic gate with optical drive was reported by us elsewhere [10].

One should note here, that the optical drive and INPUT/OUTPUT is not the only possible way of operation for a quantum dot-based logic gate. Most recently, Tanamoto suggested a quantum dot array for quantum computing with electronic drive (only electric biases are used) and INPUT/OUTPUT based on regular MOSFET [17]. The model described in Ref. [17] is similar to the single electron memory devices implemented on nanocrystals of Si [18]. The principle of operation of the quantum dot-based quantum logic gate with electronic drive is based on the following; when two dots that differ in size are coupled and one excess electron is introduced, the energy levels of the system are localized electron states with different energies. When a particular gate bias is applied, two energy states coincide and the electron transfers to another dot via resonant tunneling (electron wave function extends over two coupled dots). The state when the electron is completely localized in one dot is the computational basis state |0>. The state when the electron is completely localized in another dot is the state |1>. The estimates presented in Ref. [17], imply that under certain conditions one can maintain coherence long enough to carry out the computation despite the fact that interface traps may cause a significant problem. Both schemes, with optical drive [10] and all-electronic drive [17] that we just outlined, require very similar quantum dot structures with closely spaced quantum dots, so that Coulomb coupling is significant.

In order to prove that a quantum logic gate structure can be built using state-of-the-art technology, we have attempted to position quantum dots on the pre-patterned substrate in such a way that the dot shape and interdot spacing are kept in the required range. The structure has been fabricated using novel technique developed by the UCLA group [13] and some other research laboratories [5,6]. This technique is based on the spontaneous self-ordering of MBE grown quantum dots on a pre-patterned substrate, which we call a *cooperative assembly*. The mechanism of this self-ordering is related to the strain, and can be affected by the shape of the lithographically written pattern, growth conditions and layer thickness. In Fig. 2 we present an atomic force microscopy (AFM) picture of the self-ordered Ge quantum dots positioned on a pre-patterned Si substrate before the deposition of a cap layer. One can see that the dots are closely spaced and that their shapes are nearly identical. These two features are very important for building the quantum dot register. The smallest dot height that was obtained for these arrays is about 10 nm. It is difficult to measure exactly the base size since the dots are at the edges of the Si mesas. We estimated that the typical base size of our arrays is about 50 nm. The interdot distance, measured from center to center, in the arrays is about 100 nm. The strength of the interdot coupling can be regulated by the dot overlap on the mesa and by the choice of material for the cap layer. Although it is not shown on figure, we have also succeeded in positioning quantum dots in two-dimensional (2D) arrays with controlled interdot distance. Preliminary results have also been achieved for InAs quantum dots on Si.

The structure shown in Fig. 2 has the quality and quantum dot parameters, which are already very close to the ones required for the basic elements of a quantum dot register. Although, electronically driven scheme of Ref. [17], may require additional row of quantum dots positioned on top of initial quantum dot array. The latter can be done after deposition of the cap layer. The next steps in the fabrication of the quantum dot register are selection of the optimum material system, fabrication of the metal gate contacts and deposition of the cap layer with a low dielectric constant. Among these, one of the most difficult issues is the one related to extremely high resolution needed to place electronic gates above the quantum dots. These gates are needed to control the quantum dot (qubit) states. This issue is common for many other possible solid-state implementations of a quantum computer [4,15,21-25]. All these implementations rely on our ability to fabricate tiny metal gates and wire them either by conventional methods or using STM tips or by some even more exotic means like molecular wire connections [23,26,27]. The method of self-alignment of floating dot gate suggested by Nakajima *et al.* [28] can also be used for our structure and help to achieve the high resolution requirements.

IV. Calculation of parameters of quantum dots

The shape and the size of the quantum dots (see Fig. 2) used for a quantum register should be tuned in such a way that they have exactly two confined electron states. It is also desirable to have quantum dots made from a direct band-gap material integrated on silicon. A direct bang-gap is convenient for qubit preparation using two confined electron states and for the optical readout operation. Because of the described recent technological advances, such structure, analogous to the one shown in Fig. 2, can be fabricated on a Si substrate. Recently, one of us has reported self-assembled growth of InAs on Si (100) substrate [14]. A rather large misfit (11.5%) of this system leads to a very small dot size and inter-dot distance. The Si substrate also facilitates integration with conventional technology for electronic components.

In order to control the number of electrons in a quantum dot, we have studied electron tunneling in quantum dots both theoretically and experimentally. Using the constant interaction model, we have compared the scaling of Coulomb charging energy e^2/C with the quantum confined energy of semiconductor quantum dots

$$E_{n,k,l}{}^{e,h} = E_G + \frac{\pi^2 \hbar^2}{2m^*_{e,h}} \left(\frac{n_x{}^2}{L_x^2} + \frac{n_y{}^2}{L_y^2} + \frac{n_z{}^2}{L_z^2} \right). \tag{1}$$

Here E_G is the band gap energy and $m_{e,h}$* is the effective mass of an electron (hole), n_x, n_y, and n_z are electron and hole quantum numbers, h is the Plank's constant. Results of our numerical simulation of the energy scaling in InAs and CdS quantum dots are shown in Fig. 3. One can see from this figure that the Coulomb charging energy and the quantum confined energy are comparable for InAs quantum dots in the technologically accessible range of 100A-400A. In order to be able to see the single-electron effects in the tunneling current these energies are have to be larger than the thermal energy k_BT. This means that the gate can only operate at very low temperatures (mK – 4 K range).

Another important parameter which has to be determined for the quantum dot structure shown in Fig. 2 is an approximate value of the gate voltages (gates have to be fabricated on the top) required for controlling few electron regime. The storage of electrons in the quantum dot results in a shift in the threshold voltage of the metal-insulator-semiconductor dot device. This voltage for a single quantum dot device with n electrons in the dot is given by

$$\Delta V_T(n)=(ne/S\varepsilon_b\varepsilon_o)[(L\varepsilon_b/2\varepsilon_{InAs})+t_{top}], \qquad (2)$$

where L is the liner dimension of the quantum dot (height), S is the cross-section of the quantum dot, t_{top} is the thickness of the insulating layer, ε_b is the dielectric constant of the barrier material, ε_{InAs} is the dielectric constant of the InAs. Using numerical values characteristic for our structure (ε_{InAs}=14; t_{top}=4 nm; S=50 nm x 50 nm, L=10 nm), and assuming that the interdot space is filled with low dielectric constant material ε_b=1, we estimate $\Delta V_T(n)$ =0.32 V for n=1. If we use dielectric constant matched to InAs the voltage changes to 0.046 V. These voltages are quite realistic and can be easily supplied through the gates fabricated on top of the quantum dots.

In order to verify applicability of our structure as a quantum logic gate, we need to estimate the time during which the quantum coherence of the computational basis states is preserved. The decoherence in the case of electron charge information encoding mainly originates from interaction with the phonon bath. It is true when we use two lowest confined electron states and optical drive [3,10,15,16] as well as when only the ground state is used [11,17]. The spin-based systems have longer dephasing times and are not considered here.

We estimate the lifetime of the basic states limited by the non-radiative transitions using the well-known formalism [19]. The phonon emission rate by an electron in the state *i* is given as

$$\frac{1}{\tau_{ph}} = \frac{2\pi}{\hbar} \sum_{f,q} \alpha^2(q) |< \Psi_f | e^{-iqr} | \Psi_i >|^2 \delta(E_f - E_i + E_q)[N_o(T, E_q) + 1], \quad (3)$$

where the sum extends over all possible final-electron quantum numbers *f* and phonon wave vectors q, $N_0(T, E_q)$ is the Bose-Einstein distribution function, E_q is the energy of a phonon with wave vector q, T is the temperature, and α is the coupling constant. An analogous expression can be written for phonon absorption [19]. One has to consider the coupling of electrons to longitudinal acoustic (LA) phonons via deformation potential and the Frohlich interaction between the electron and longitudinal optical (LO) phonons. These two mechanisms are expected to be dominant for our structures although much weaker than in the bulk. Interaction with longitudinal optical phonons in the quantum dot structure occurs when the level separation is close to the LO phonon energy $\hbar\omega_{LO}$. The expressions for the coupling constants are given in Ref. [19]. We perform the calculations with the material parameters, which correspond to InAs/Si system. The numerical simulation for T=4 K shows that τ_{ph} is on the order of 1-10 ns for a 10 nm high quantum dot structure with 50 nm square base.

A possible presence of interface traps is another issue of concern. However, the density of trap states can be smaller (~10^{10} cm^{-2}) than the density of self-assembled dots (~10^{12} cm^{-2}). The quantum dot array structure suggested by us as a prototype for the quantum dot register is fabricated using self-assembly and self-ordering procedure rather then lithography. The latter helps to minimize the number of interface traps. Fabricating the quantum dot structure by the method of cooperative self-assembly, we have used conventional lithography only to define the size of the mesa structure but not the dot sizes, which can be much smaller. This allowed us to have small and high quality self-assembled dots positioned in predetermined locations.

Some recent studies suggested that the phase coherence time in the mesoscopic systems should saturate at a finite temperature due to the zero-point fluctuations of the phase coherent electrons [20]. This means that the coherence time can not be significantly increased even if the temperature approaches zero. The temperature at which this saturation occurs varies by orders of magnitude ranging from few mK to 10 K. Thus, even if we suppress dephasing due to coupling to phonon bath, the coherence time will still be limited by the zero-point fluctuations. Ref. [20] provides experimental and calculated values of the phase coherence time limited by this mechanism, which are on the order of τ_{coh} ~ 0.1-4 ns depending on the material parameters.

If the electric field is used for level tuning (via Stark shift) and for performing the computation, one has to estimate time-delay required for adiabatic switching. With current techniques, one can vary or sweep electric field in a time scale of picoseconds. One can also estimate the time τ_δ required for charge transfer in coupled quantum dots using the model of Refs. [11,17] as

$$\frac{1}{\tau_\delta} = \frac{8}{\pi\hbar}\left(\frac{V_o - E}{V_o}\right)\frac{E}{1 + Kl_\omega} e^{-Kl_d},$$

where l_w is the width of the quantum dot, l_d is the width of the barrier between the dots, V_o is the barrier height, E is the electron energy, and $K=(8\pi^2 m(Vo-E)/h^2)^{1/2}$. For a given material system and structure parameters this time is also on the order of picosecond. This is faster than the decoherence time.

If the optical drive is used as suggested in Ref. [10], one should be able to do the computation using femtosecond laser technology. If the π pulse duration τ_π is on the order of femtosecond and the decoherence time in on the order of nanosecond, one still can do $N \sim \tau_{coh}/\tau_\pi = 10^6$ computations. If the electronic drive is used, the time required for each computation step is on the order of picosecond. In this case, the number of possible computation steps $N \sim \tau_{coh}/\tau_\delta = 10^3$.

As we pointed out in the introduction, the proposed structure can also be used as a basic element for quantum logic gates that use electron spins as computational basis. In this case we can much easier satisfy the coherency requirements, but will have to deal with more stringent requirements for addressing of individual qubits and the problem of closer spacing of the quantum dots. These are exactly the issues, which proposed method of fabrication (self-ordering of quantum dots on pre-patterned substrates) and proposed quantum dot structure can help to solve. The small fluctuations in the size of self-assembled quantum dots can be corrected by application of particular gate voltage during the initialization procedure.

V. Conclusion

We have presented a quantum dot structure fabricated by lithographic positioning, which can be used as a prototype of the quantum dot register for quantum computing. The parameters of the fabricated quantum dot structure are very close to the ones required for two possible embodiments of a quantum computer (with optical drive and electronic drive). Simple estimates of the coherency time of the system and required gate biases are also given. Currently, we carry out experiments on controlling the number of electrons and confined levels in such a structure, which are required for the gate operation.

Acknowledgement

One of the authors (AB) thanks Dr. S. Bandyopadhyay (UNL) for valuable comments on the coherence time in memsoscopic systems. The authors thank Ms. Zina Romero for her help in manuscript preparation.

References

1. D. Deutsch, *Proc. R. Soc. Lond.*, A **400**, 97 (1985).
2. D. Loss and D.P. DiVincenzo, *Phys. Rev. A*, 57, 120 (1998).
3. A. Balandin and K.L. Wang, *Superlatt. and Microstruct.*, **25**, 509 (1999).
4. B.E. Kane, *Nature* **393**, 133 (1998).
5. T.I. Kamins, R.S. Williams, *Appl. Phys. Lett.*, **71**, 1201 (1997).
6. T.I. Kamins, R.S. Williams, *Surface Science*, **405**, L580 (1998).
7. N.H. Bonadeo, G. Chen, D. Gammon, D.S. Katzer, *Phys. Rev. Lett.*, **81**, 2759 (1998).
8. N.H. Bonadeo, J. Erland, D. Gammon, D. Park, *Science*, **282** (5393), 1473 (1998).
9. L. Kouwenhoven and C. Marcus, *Physics World*, June 1998, p. 35; R.C. Ashoori, *Nature*, **379**, 413 (1996); S. Tarucha, D.G. Austing, T. Honda, R.J. van der Hage, L.P. Kouwenhoven, *Phys. Rev. Lett*. **77**, 3613 (1996).
10. Balandin and K.L. Wang, in *Quantum Computing and Quantum Communication*, Lecture Notes in Computer Science, Vol. **1509** (Springer-Verlag, Berlin Heidelberg, Germany, 1999), edited by C.P. Williams, pp. 460-467.
11. T. Tanamoto, “Quantum computation by coupled quantum dot system and controlled NOT operation,” LANL quant-ph/9902031.
12. G. Burkard, D. Loss, and D. DiVincenzo, “Coupled quantum dots as quantum gates,” LANL cond-mat/9808026.
13. G. Jin and K.L. Wang, *Appl. Phys. Lett*, to appear.
14. C. Sharma, K.W. Alt, D.Y. Yeh, D. Wang, and K.L. Wang, *J. Electron. Materials*, **28**, 432 (1999).
15. A. Barenco, D. Deutsch, A. Eker, R. Jozsa, *Phys. Rev. Lett*. **74**, 4083 (1995).
16. S. Bandyopadhyay, A. Balandin, F. Roychowdhury, F. Vatan, *Superlatt. Microstruct*. **23**, 445 (1998).
17. T. Tanamoto, “Quantum gates by coupled quantum dots and measurement procedure in Si MOSFET,” LANL quant-ph/9908021.
18. S. Tiwari, F. Rana, H. Hanafi, A. Hartstein, E.F. Crabbe, K. Chan, *Appl. Phys. Lett.*, **68**, 1377 (1996).
19. U. Bockelmann and G. Bastard, *Phys. Rev. B*, **42**, 8947 (1990).

A. Balandin, G. Jin, and K.L. Wang, *J. Electronic Materials*, **29**, 549-553 (2000).

20. P. Mohanty, E.M.Q. Jariwala, and R.A. Webb, *Phys. Rev. Lett.*, 78, 3366 (1997).
21. N.-J. Wu, M. Kamada, A. Natori and H. Yasunaga, “Quantum computer using coupled quantum dot molecules,” LANL quant-ph/9912036.
22. P. Zanardi and F. Rossii, *Phys. Rev. B*, **59**, 8170 (1999).
23. S. Bandyopadhyay, “A self-assembled nanoelectronic quantum computer based on the Rashba effect in quantum dots,” LANL quant-ph/9910032.
24. R. Vrijen, E. Yablonovitch, K.L. Wang, H.W. Jiang, A. Balandin, V. Roychowdhury, T. Mor, and D. DiVincenzo, “Electron spin resonance transistors for quantum computing in silicon-germanium heterostructures,” LANL quant-ph/9905096.
25. V. Privman, I.D. Vagner, and G. Kventsel, “Quantum computation in quantum-Hall system,” LANL quant-ph/9707017.
26. J.M. Tour and J.S. Schumm, *Pol. Prep*., **34**, 368 (1993).
27. R.P. Anders, *et. al*., *Science,* **273**, 1690 (1996).
28. A. Nakajima, T. Futatsugi, K. Kosemura, T. Fukano, and N. Yokoyama, *App. Phys. Lett.*, **70**, 1742 (1997)

FIGURE CAPTUNS

1. Schematic picture of a quantum dot register for quantum computing. The gates are used to control the number of electrons in the dots, and for adjustment of the level spacing via Stark shift. In the optically driven gates, the computation is performed via application of π pulses, while in the electronically driven gates, it is performed via modulation of the gate potentials. The inset shows confined electron levels that form a qubit.

2. Atomic force microscopy (AFM) picture of the prototype structure with self-ordered Ge quantum dots positioned on a pre-patterned Si substrate. It is possible to control the size of the dots, their shape and interdot distance by varying the lithographic pattern and growth conditions.

3. Scaling of the Coulomb charging energy and quantum confinement energy in InAs and CdS quantum dots. Depending on the shape of the InAs dots and interdot spacing, these two energies can be made equal in the convenient range of 100 A - 500 A.

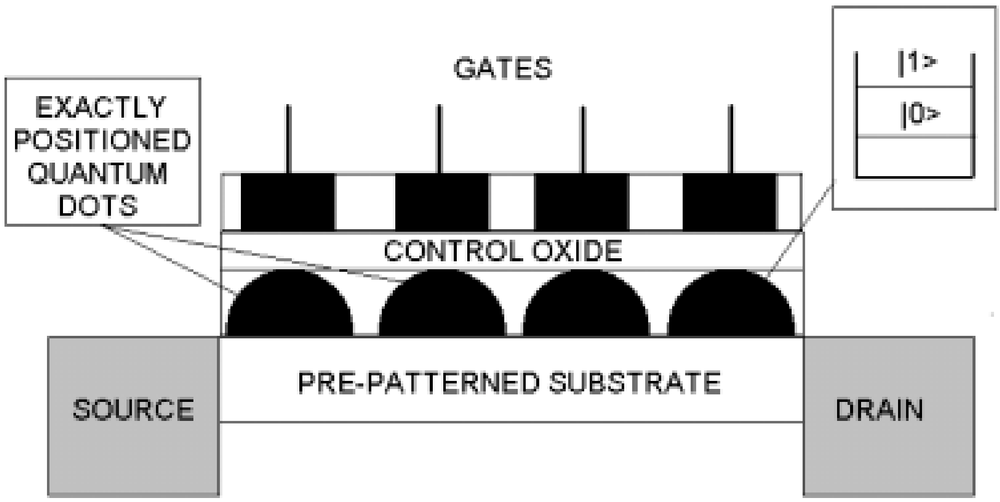

Figure 1. A. Balandin, G. Jin and K.L. Wang, JEM

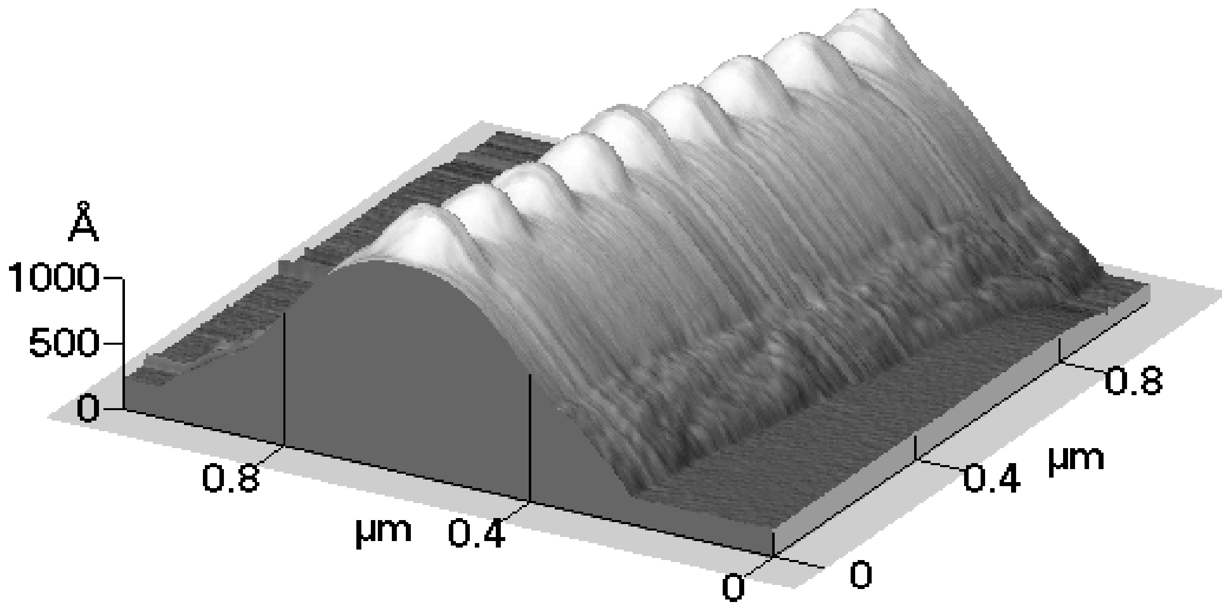

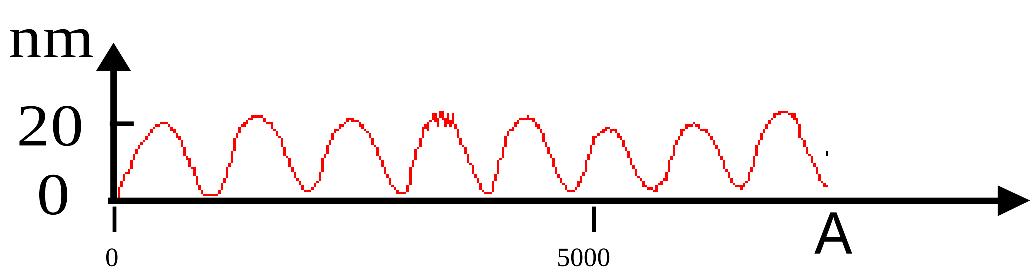

Figure 2. A. Balandin, G. Jin and K.L. Wang, JEM

A. Balandin, G. Jin, and K.L. Wang, *J. Electronic Materials*, **29**, 549-553 (2000).

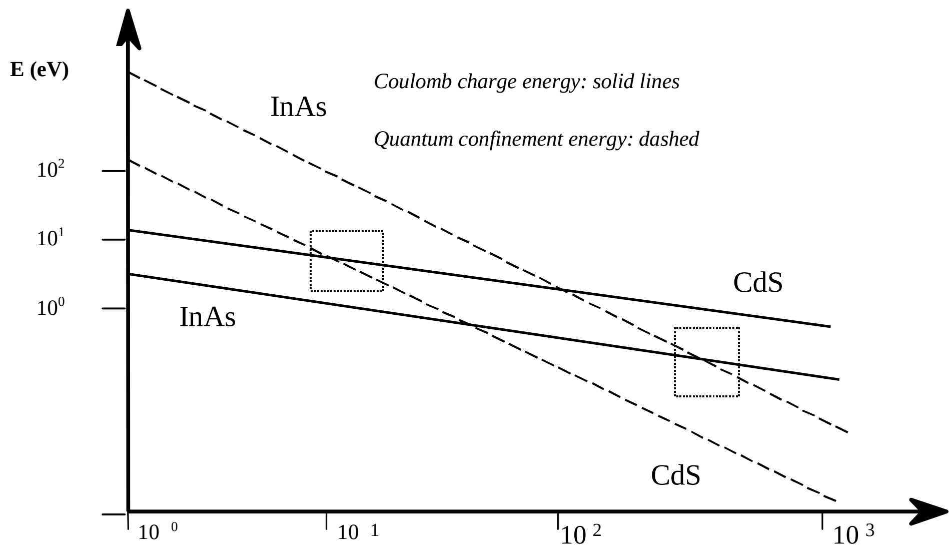

Figure 3. A. Balandin, G. Jin and K.L. Wang, JEM